

TABLE OF CONTENTS

FIGURES AND TABLES	2
1. INTRODUCTION	3
2. SITE GEOLOGY	3
2.1 Geology History Overall.....	3
2.2 Landslide Site Geology.....	3
2.3 Soil/Rock Formation.....	4
2.4 Groundwater	4
3. MODEL SETUP IN SLIDE 7.0	5
3.1 Model Material Properties	6
3.2 Model Groundwater	8
3.3 Model Tension Crack.....	9
3.4 Model Failure Surface.....	9
4. SENSITIVITY ANALYSIS	10
4.1 Sensitivity of Soil Strength Parameters	10
4.2 Sensitivity of Groundwater Conditions	13
4.3 Sensitivity of Tension Crack Properties	14
4.4 Sensitivity of Varying Bedding Planes.....	15
5. PROBABILISTIC ANALYSIS.....	15
6. MITIGATION METHOD	16
7. SEISMIC HARZARD ANALYSIS	18
7.1 Static Analysis	18
7.2 Pseudo-static Analysis	19
7.3 Displacement-Based Analysis	20
REFERENCES	22
APPENDIX	23

FIGURES AND TABLES

Figure 1 Shannon & Wilson White Point Section CC'	5
Figure 2 Initial Model Setup, Section CC'	6
Figure 3 Residual Shear Strength of Bentonite Clay	8
Figure 4 Initial Model Result with FS Close to Unit	9
Figure 5 Tma Properties Sensitivity Plot	11
Figure 6 Bentonite Clay Shear vs. Normal Stress.....	12
Figure 7 Bentonite Clay Friction Angle Sensitivity Plot.....	12
Figure 8 Piezometric Line Sensitivity Plot.....	13
Figure 9 Tension Crack Sensitivity Plot.....	14
Figure 10 Bedding Inclination Sensitivity Plot.....	15
Figure 11 Probabilistic Analysis.....	16
Figure 12 Mitigation Method Analysis.....	17
Figure 13 Coordinates of New Fill in Slide7.0.....	18
Figure 14 Ky of Static Analysis.....	19
Figure 15 Factor of Safety for Pseudo-static Analysis	20
Figure 16 Sa(g) vs. Ts(s) for Cabrillo fault.....	21
Figure 17 Excel for Calculation of Seismic Displacement.....	21
Table 1 Material Properties used in Model.....	7
Table 2 Tma Material Property Range for Sensitivity Analysis.....	10
Table 3 Determination for m & s Range.....	10
Table 4 Piezometric Line Parameters Range for Sensitivity Analysis	13
Table 5 Seismic Displacement and Corresponding Probability	21

1. INTRODUCTION

This report includes geological information, Slide7.0 model analysis results, and restoration suggestions for the landslide happened at White Point, San Pedro District, Los Angeles, on January 6, 2012. Before the landslide, movements of ground are continuously observed by City of Los Angeles representatives since 2010. Cracks and displacements kept increasing and finally led to the happening of this failure.

2. SITE GEOLOGY

The Palos Verdes Peninsula is famous for landslide due to historical and geological reasons. The happening of White Point Landslide is not an uncommon case.

2.1 Geology History Overall

Palos Verdes Peninsula was formed by the compression of tectonic plates, which uplifts the area continuously and this action created anticline beds consist of marine and alluvial soil. Faults related to this area are the Palos Verdes Fault and the Newport-Inglewood Fault, most importantly, the bed inclination paralleled with the Palos Verdes Fault. Therefore, as the uplift speed is not uniform, when the rising of the earth is too fast the land will slide down as the potential energy of gravity overcomes the inertial cohesion of the rock and soil.

2.2 Landslide Site Geology

It is observed that bedding attitudes along the beach and outside the landslide mass shows a synclinal structure, and its axis oriented from north to south into the Pacific Ocean. This syncline probably acts as a major reason for the White Point Landslide. The western dip of this fold range from 14 to 31 degrees SE, while the eastern part dip between 9 to 14 degrees. With exploration data from site, bedding strike attitudes range from east side (landslide headscarp) N44°W to the west side N73°E and N27°E. Dip angle at south side is 12 to 35°.

At west part of the landslide, there are mainly two structure types. One is a tight isoclinal folds with east-west fold axes, another is the same folds with northwest-southeast fold axes. Many of these two structures can be observed along the sea cliff facing west of the main landslide mass. The boundary of these two structure is a group of northeast shears or faults that parallel with the western boundary of the active landslide scarp.

2.3 Soil/Rock Formation

In case of the White Point Landslide, the most critical character is the property of Monterey Formation. It is an extensive Miocene oil rich geological sedimentary formation, and it's categorized into 3 parts in the report: the Altamira Shale (Tma), the Valmonte Diatomite and the Malaga Mudstone, among which the Altamira Shale is of the most importance.

In the lower part of the Altamira Shale, tuffaceous lithofacies dominates. This rock material was formed initially by volcanic ash and cinder, and when interact with water, it transforms into bentonite clay. Bentonite swells when in contact with water and becomes greasy, which creates a weak layer for slides to happen. As shown by boring results, the critical bentonite bed that is wet, soft and polished lay at 88 to 97 feet below ground, while other bentonite layers do not show the propensity to cause failure. Therefore, this critical bentonite layer separates the Altamira Shale into two layers, upper layer being oxidized while the lower layer exhibits rock-like property which acts as bedding.

Furthermore, the bedding plane of the anticline paralleled with the layer, which enlarged the tendency for the slope to fail. Thirdly, the layout of the rock as jagged masses or sea stacks also added the proneness to slide as the wave action by the shoreline continued to cut into the base.

Lastly, above the Altamira Shale, a layer of quaternary marine and non-marine terrace deposits (Qt) is observed all over the site and range in 4.5 to 9 feet deep. The desiccation cracks and moisture content of the soil shows a sign of expansive, plastic clay.

Subsurface profiles were interpreted by site data and subsurface samples. Among all the sections drawn, section C-C' was approximately parallel to the direction of landslide. So, the model prepared in Slide7.0 will be referring to this section.

2.4 Groundwater

Historically, excess hydrostatic pressure is observed near the site and this contributes to the landslide because of lower effective vertical stress, lower shear strength and greater uplift pressure. Proof of artesian groundwater were found when the water surface rised significantly after one day at some drilling wells across the site. Furthermore, some boring locations even encountered flowing artesian condition where the hydrostatic pressures forced groundwater flow above the ground surface. It is deduced that the confined acquifer which led to flowing artesian is related to

the bentonite clay layer found from the boring samples which located at the elevation of 88 to 97 feet.

3. MODEL SETUP IN SLIDE 7.0

Numerical models are set up to perform the stability analysis. With information obtained on site, soil properties and groundwater conditions are set to reproduce the landslide failure which is the back-analysis method. The model geometry is based on Shannon & Wilson White Point Final Plates section CC' (as shown in Figure 1), since this is the section that coincided with slide direction and also representative with a proper range of geology and hydrology configuration. Model setup is shown in Figure 2.

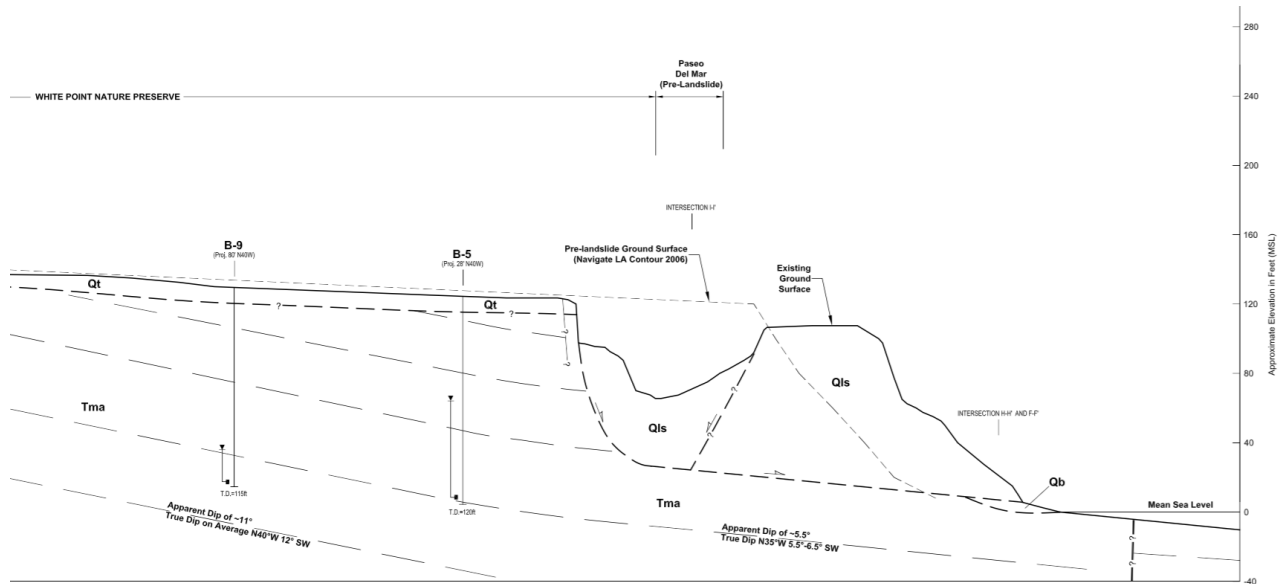


Figure 1 Shannon & Wilson White Point Section CC'

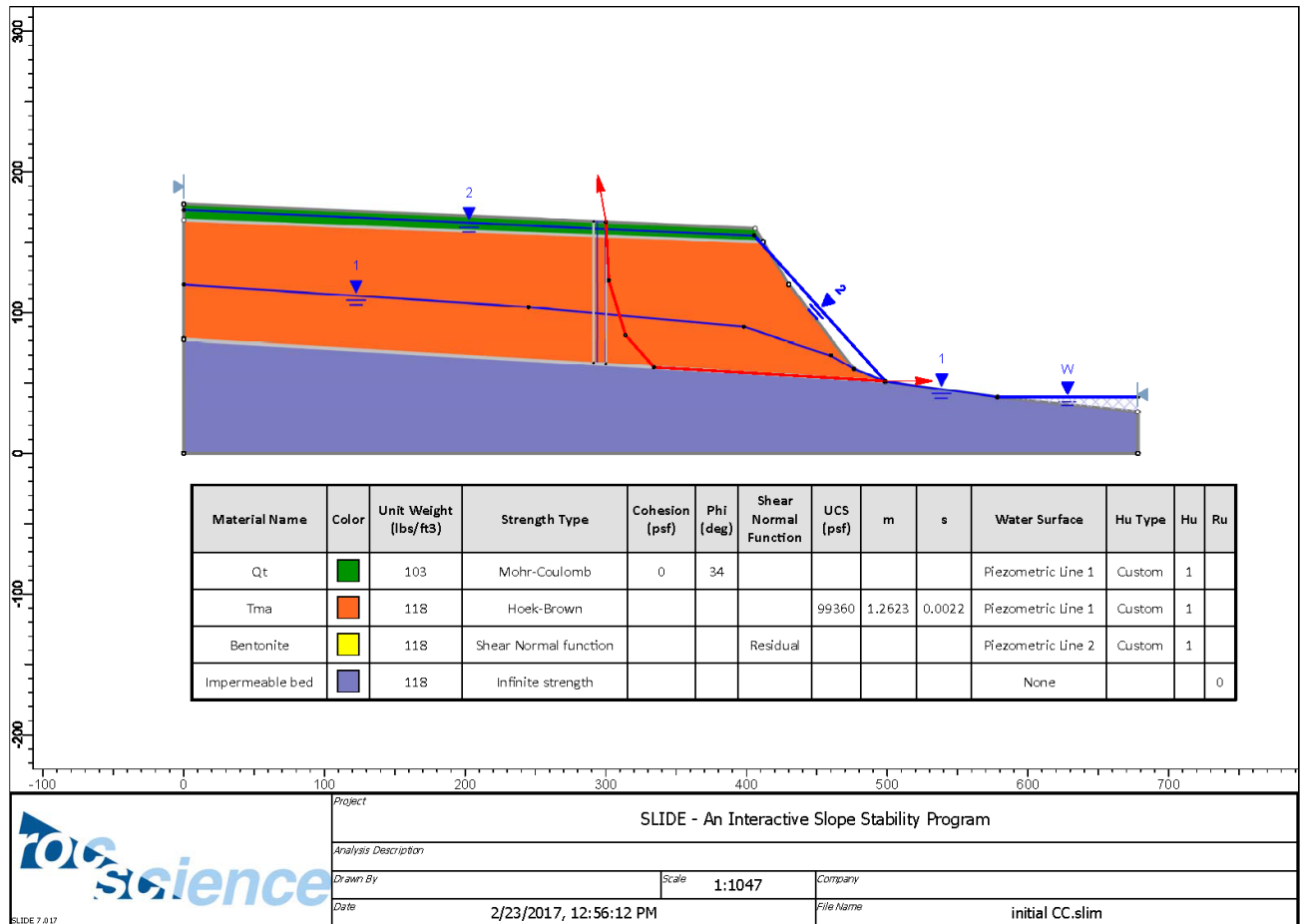


Figure 2 Initial Model Setup, Section CC'

3.1 Model Material Properties

For soil parameters, data from White Point Final Main Body is used as presented in Table 1.

Table 1 Material Properties used in Model

Unit	Strength Model	Total Unit Weight pcf ¹	Friction Angle degrees	Cohesion psf ²	Uniaxial Compressive Strength psi ³	Geologic Strength Index ⁴	Intact Rock Parameter ⁴ , m_i	Disturbance Factor ⁴ , D
Terrace Deposits (Qt)	Mohr-Coulomb	103	34	0	NA	NA	NA	NA
Altamira Shale (Tma)	Hoek-Brown ⁵	118	See Note 5	See Note 5	690	45	9	0
Weathered Tuff (Bentonite Clay; Tma)	User-Defined Nonlinear Function ⁶	118	See Note 6	See Note 6	NA	NA	NA	NA

Notes:

1. pcf = Pounds per cubic foot
2. psf = Pounds per square foot
3. psi = Pounds per square inch
4. As described by Hoek and Marinos (2000).
5. The generalized Hoek and Brown (1997) model is nonlinear and does not correspond to single values of friction angle and cohesion; the full nonlinear curve is presented in Appendix G.
6. The shear strength envelope used to model the bentonite clay is nonlinear and does not correspond to single values of friction angle and cohesion; the full nonlinear curve is presented in Appendix G.

For Altamira Shale (Tma), Hoek-Brown relationship is used, as this relationship counts for non-linear strength relationship instead of using only one set of cohesion and friction angle to characterize the soil.

Parameter m and s are calculated based on provided Geologic Strength Index (GSI) and Intact Rock Parameter (m_i). From Rocscience document “Rock Mass Properties”, formulas can be found as:

$$m_b = m_i \exp\left(\frac{GSI - 100}{28 - 14D}\right)$$

$$s = \exp\left(\frac{GSI - 100}{9 - 3D}\right)$$

Where D varies from 0 to 1 depends on the degree of disturbance due to blast damage and stress relaxation. Since on site there is no blast damage of rock mass, D is set to be 0.

For the Bentonite Clay Layer, which is the weakest failure plane, properties are based on lab test results from White Point Final Appendix G. To be conservative, the residual shear strength is used, and the related graph is presented in Figure 3. Data points are read from the graph and input into Slide as ‘Shear Normal Function’. Furthermore, in the model layer thickness is set to be 0.5 ft.

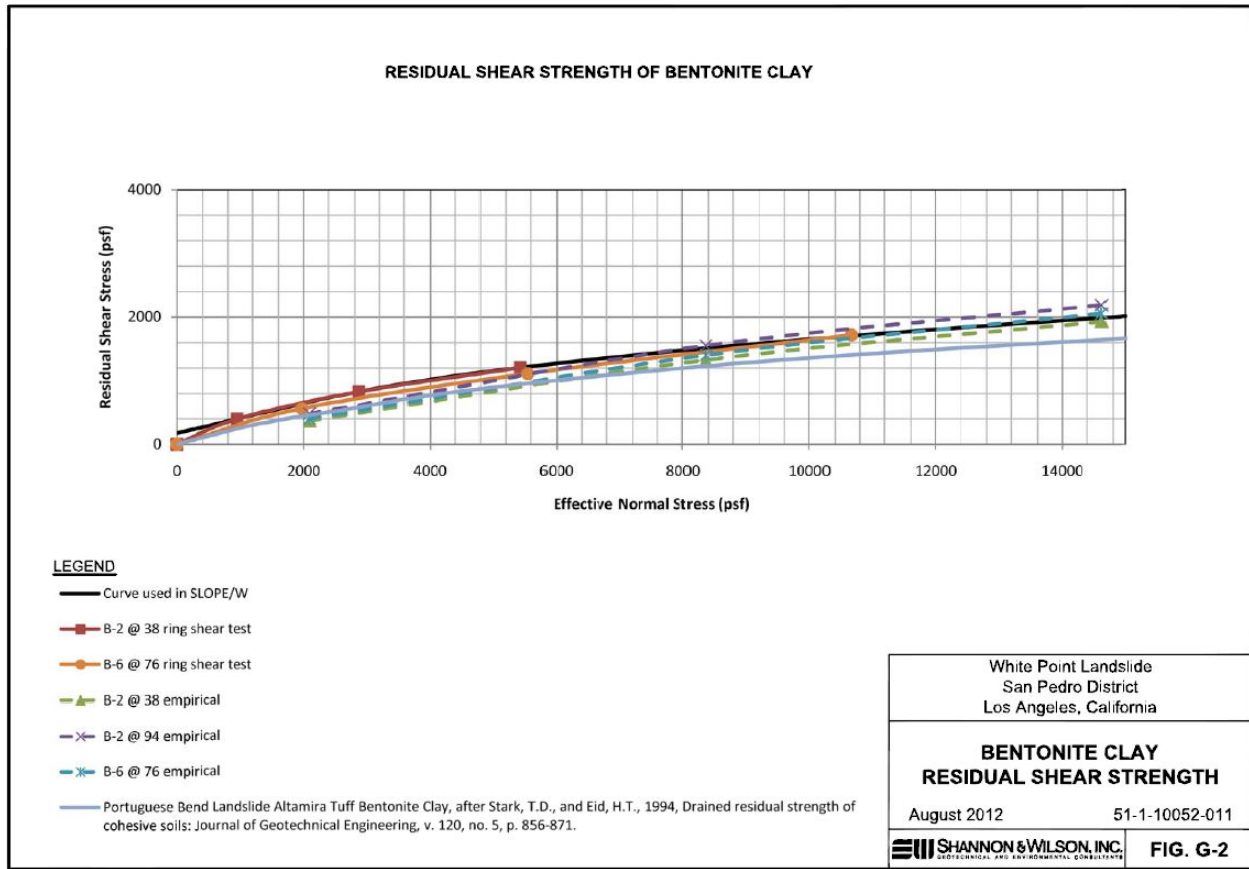


Figure 3 Residual Shear Strength of Bentonite Clay

As the bedding material below the bentonite clay, not much oxidation happened as mentioned previously and strength is preserved to be larger than the oxidized Tma above. Here an impermeable property is assigned to it so the failure will be forced to fail through the bentonite clay.

Terrace deposit (Qt) at the site surface is presented with Mohr-Colomb relationship with $c=0$ and $\phi=34^\circ$. As is found from ground survey across the site, this layer has a thickness of 4.5 to 9 feet, in the model it is set to around 9ft.

3.2 Model Groundwater

Two piezometric lines are set according to site conditions. As the bentonite clay layer is found to have excessive hydrostatic pressure and certain location with flowing artesian situation, a high piezometric line 2 is set only for the bentonite clay layer, while piezometric line 1 of a lower height is set for the rest material.

3.3 Model Tension Crack

As cracks were observed continuously through the failure process, tension crack filled with water was introduced into the model just behind the predicted failure surface, as this can be a significant trigger factor for the landslide. Besides that, local weather and environmental conditions also indicate constant dry and wet cycles for top soil due to rain and irrigation.

3.4 Model Failure Surface

As back analysis method is implemented, the known failure surface is approximated in the model with a non-circular failure surface. The bottom of the failure surface goes through the mid of clay layer and other parameters are adjusted to reach a unit factor of safety which indicates the happening of slide.

Model results are presented below

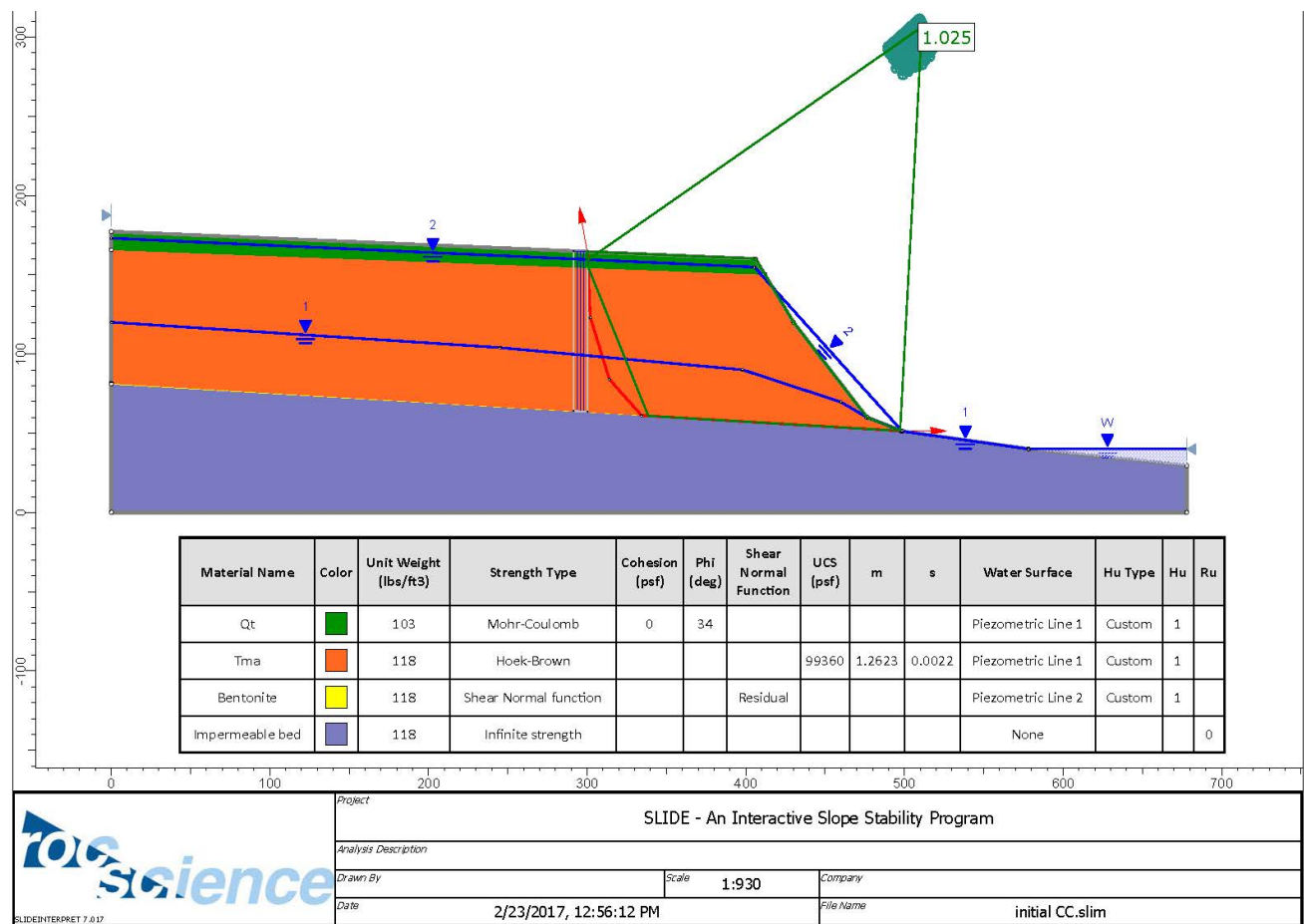


Figure 4 Initial Model Result with FS Close to Unit

4. SENSITIVITY ANALYSIS

4.1 Sensitivity of Soil Strength Parameters

Range of Altamira Shale Properties are listed below:

- **UCS:** Uniaxial Compressive Strength
- **m:** equal to m_b where calculation is mentioned previously. This is a derived value from Hoek-Brown constant Intact Rock Parameter(m_i) for the rock mass and Geologic Strength Index (GSI).
- **s:** constant which depend on GSI.

Table 2 Tma Material Property Range for Sensitivity Analysis

Material Property	Mean	Standard Deviation	Rel. Max/Min
Tma - UCS(intact)	99360	14400	43200
Tma - m	1.262	0.24	0.72
Tma - s	0.002218	0.0007	0.0021

The range of UCS varies from 450 to 1050 psi, which is 64800 to 151200 psf. As the initial value is 690 psi (99360 psf), standard deviation and relative maximum and minimum are calculated.

Based on report of Shannon & Wilson and basic rock properties, GSI are set to vary between a range of 30 to 60, accordingly, m and s parameters are calculated and related values are presented below:

Table 3 Determination for m & s Range

	GSI=30	GSI=60	Std. Dev	Rel. Max./Min.
m	0.738	2.157	0.236	0.709
s	0.000419	0.01174	0.00189	0.00566

Sensitivity analysis result from Slide is shown below:

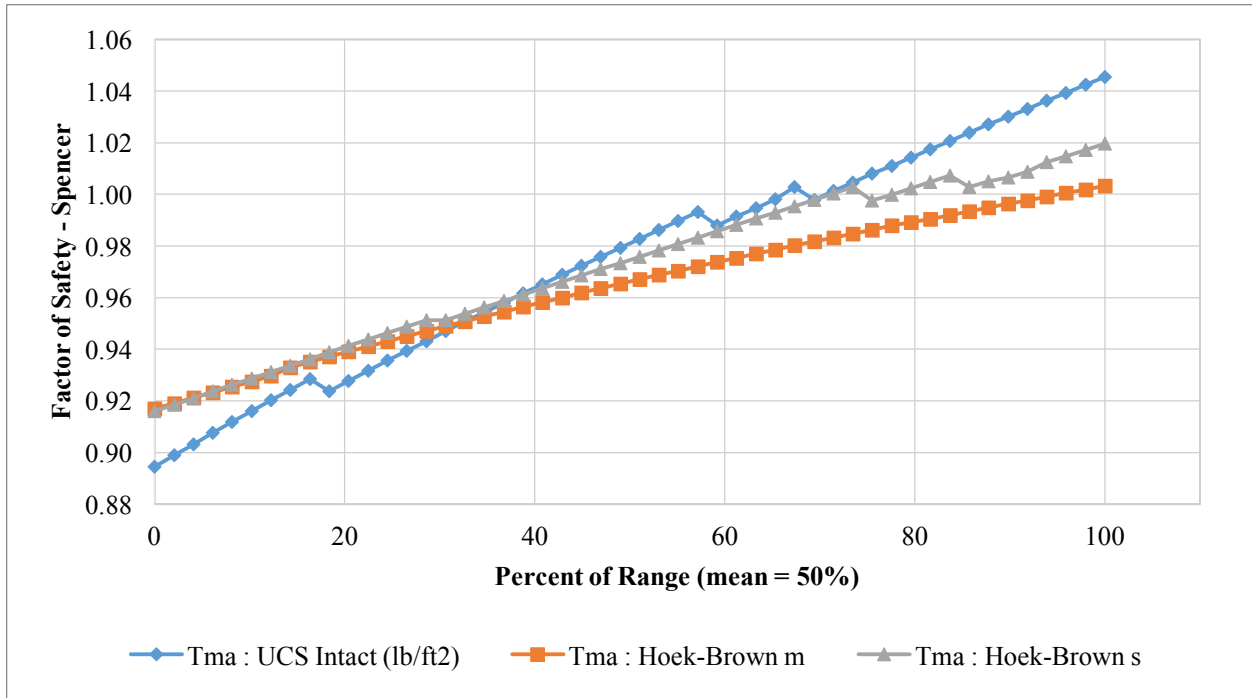


Figure 5 Tma Properties Sensitivity Plot

As can be seen from the graph, factor of safety all increased as the parameters increase. As m and s are derived parameters from GSI and m_i , and they are all positively related, it can be deduced that as UCS , GSI , or m_i increase, Factor of safety will increase. Overall, these trends indicated that as the soil mass has higher strength, or more homogeneous, it is less prone to landslide failure.

For the Bentonite Clay, shear and normal residual stresses are interpreted below in the figure and a linear trend line is drawn to find the approximate cohesion and friction angle so as to do sensitivity analysis in slide. $C = 300$ psf and $\phi = 7^\circ$ are used in the model with a variation of 3° to maximum and minimum value. The extrapolation figure and result figure from Slide are presented below.

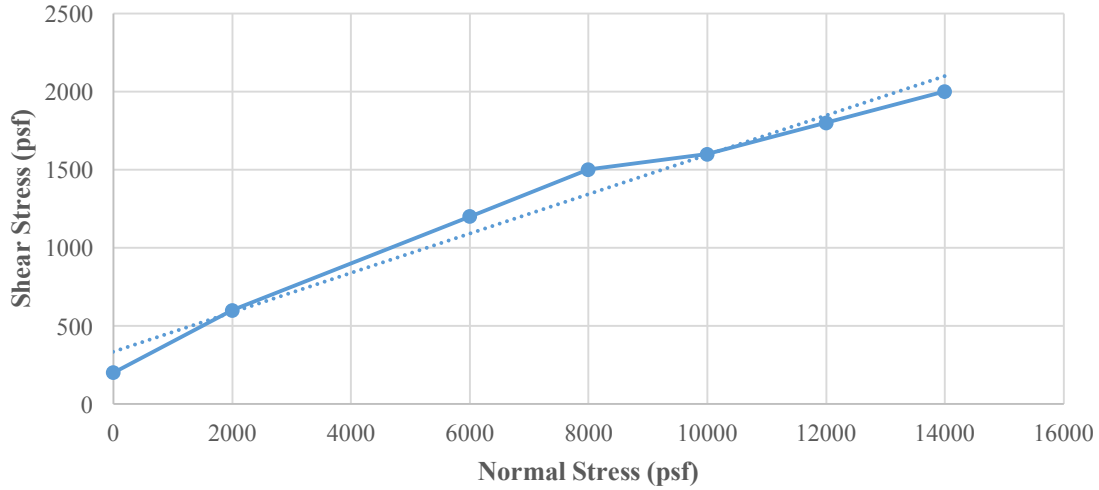


Figure 6 Bentonite Clay Shear vs. Normal Stress

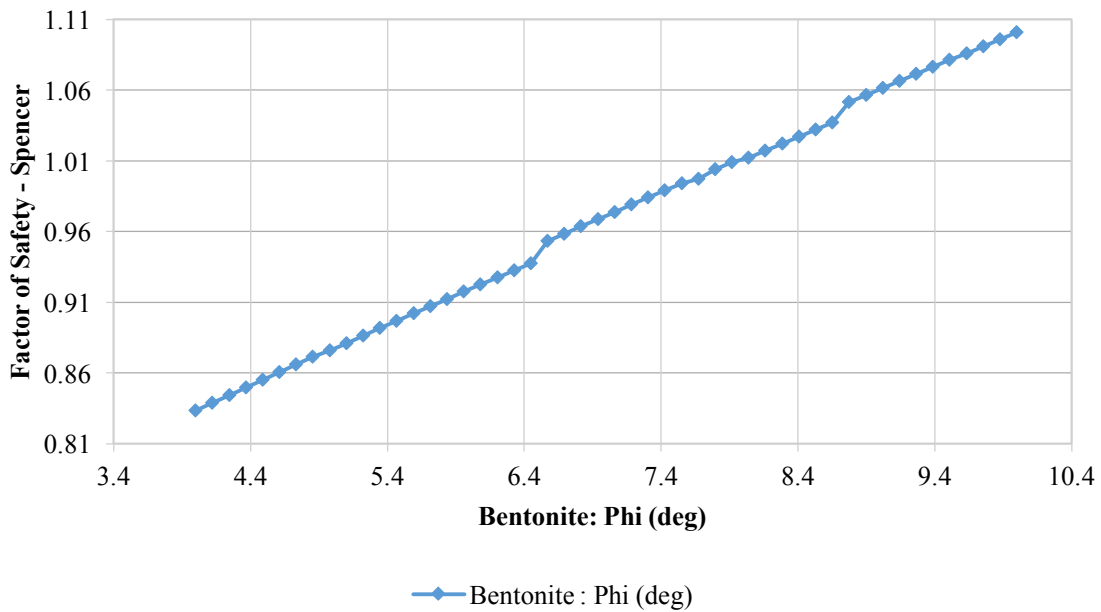


Figure 7 Bentonite Clay Friction Angle Sensitivity Plot

Conclusion can be drawn that as the friction angle increase, factor of safety increases significantly since the bentonite clay layer is the weakest plane and slight variation can mean big effect.

4.2 Sensitivity of Groundwater Conditions

Variations of piezometric lines are listed below in the table:

Table 4 Piezometric Line Parameters Range for Sensitivity Analysis

Piezometric Line Number	Pressure Head Std. Dev.	Rel. Max./Min.
1	15	45
2	3	9

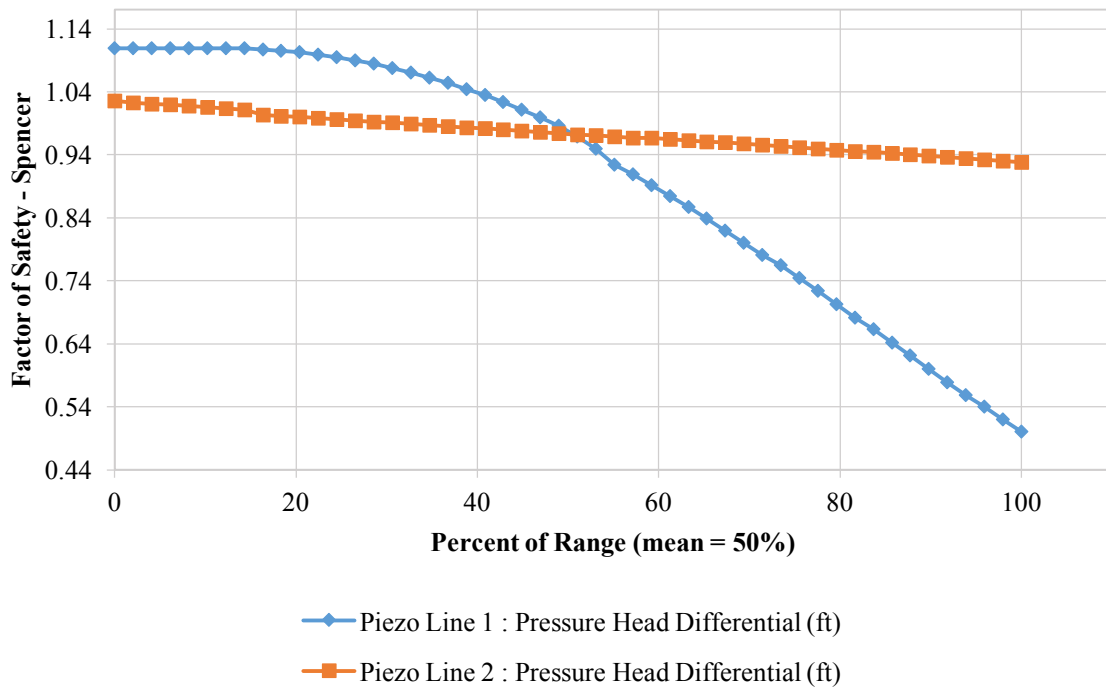


Figure 8 Piezometric Line Sensitivity Plot

From the graph it is obvious that piezometric line 2 does not affect factor of safety as much as piezometric line 1. Variations of piezometric line 1 has a larger range since position of this water table has more room and the irregular weather and local environment can cause the value to vary from time to time. As for the confined aquifer, variation cannot be attained from surface infiltration but only from below the bentonite layer, so the range of variation is smaller.

4.3 Sensitivity of Tension Crack Properties

For the tension crack, percentage fill of water is varied from 5% to 95% for sensitivity analysis, and result is shown below:

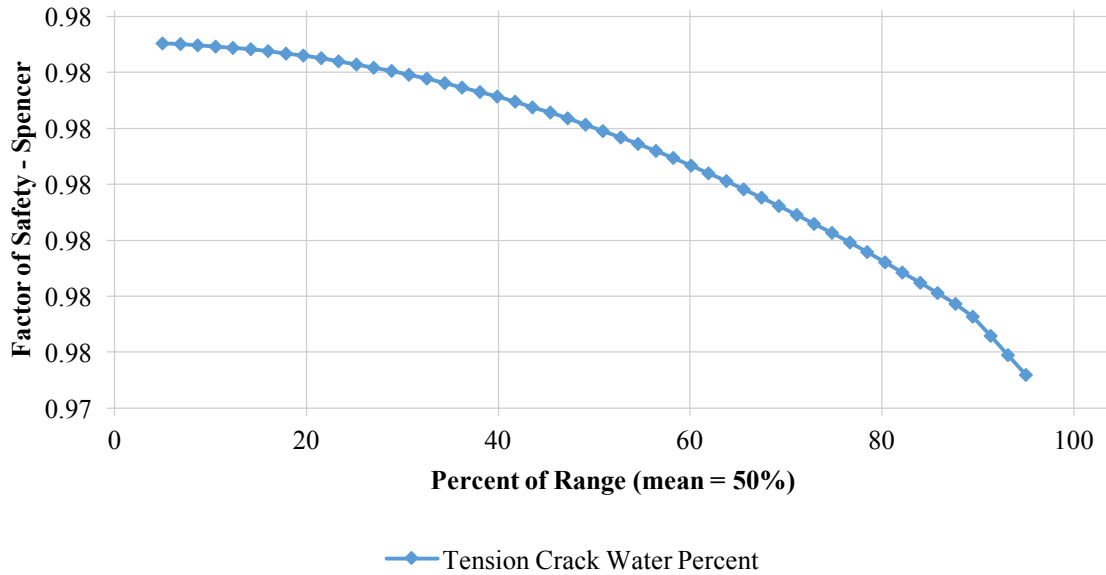


Figure 9 Tension Crack Sensitivity Plot

As can be seen the variation is very small for factor of safety (change < 0.01), although it tends to decrease factor of safety, it is not a crucial factor to cause landslide.

4.4 Sensitivity of Varying Bedding Planes

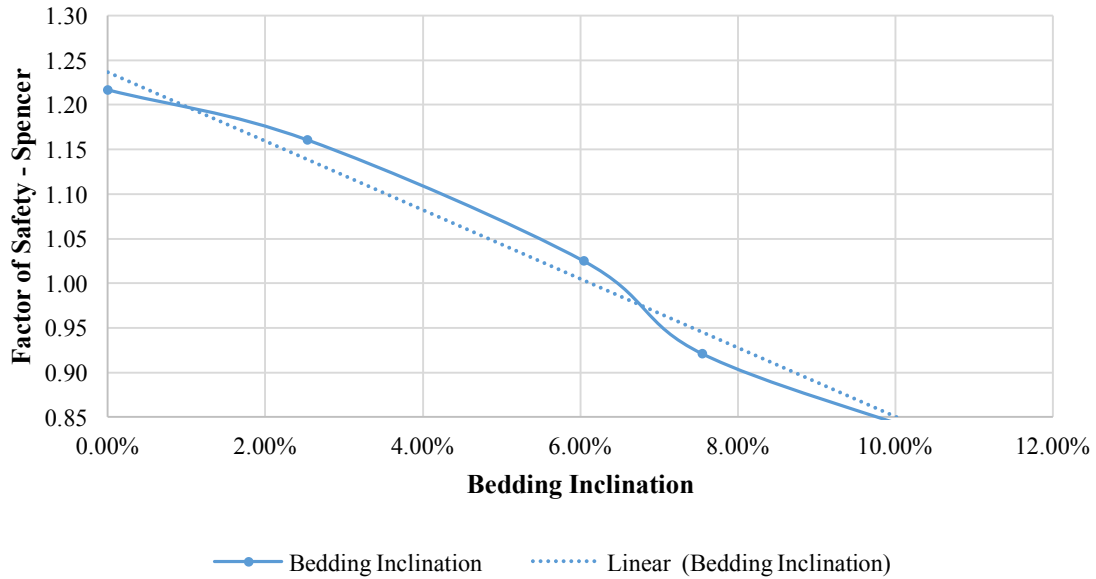


Figure 10 Bedding Inclination Sensitivity Plot

From the graph, the steeper the bedding plane, the lower is the factor of safety because of the larger gravity component along the failure surface. Detailed results are shown in Appendix

5. PROBABILISTIC ANALYSIS

Probabilistic analysis is then carried out with Monte-Carlo method, 1000 samples and Global Minimum analysis type. With the same parameters variation range defined for sensitivity analysis, the probability of failure (PF) is 53.799% as shown below. Therefore, the probability of failure is more than half which indicated that with the current model parameters the slope is prone to failure.

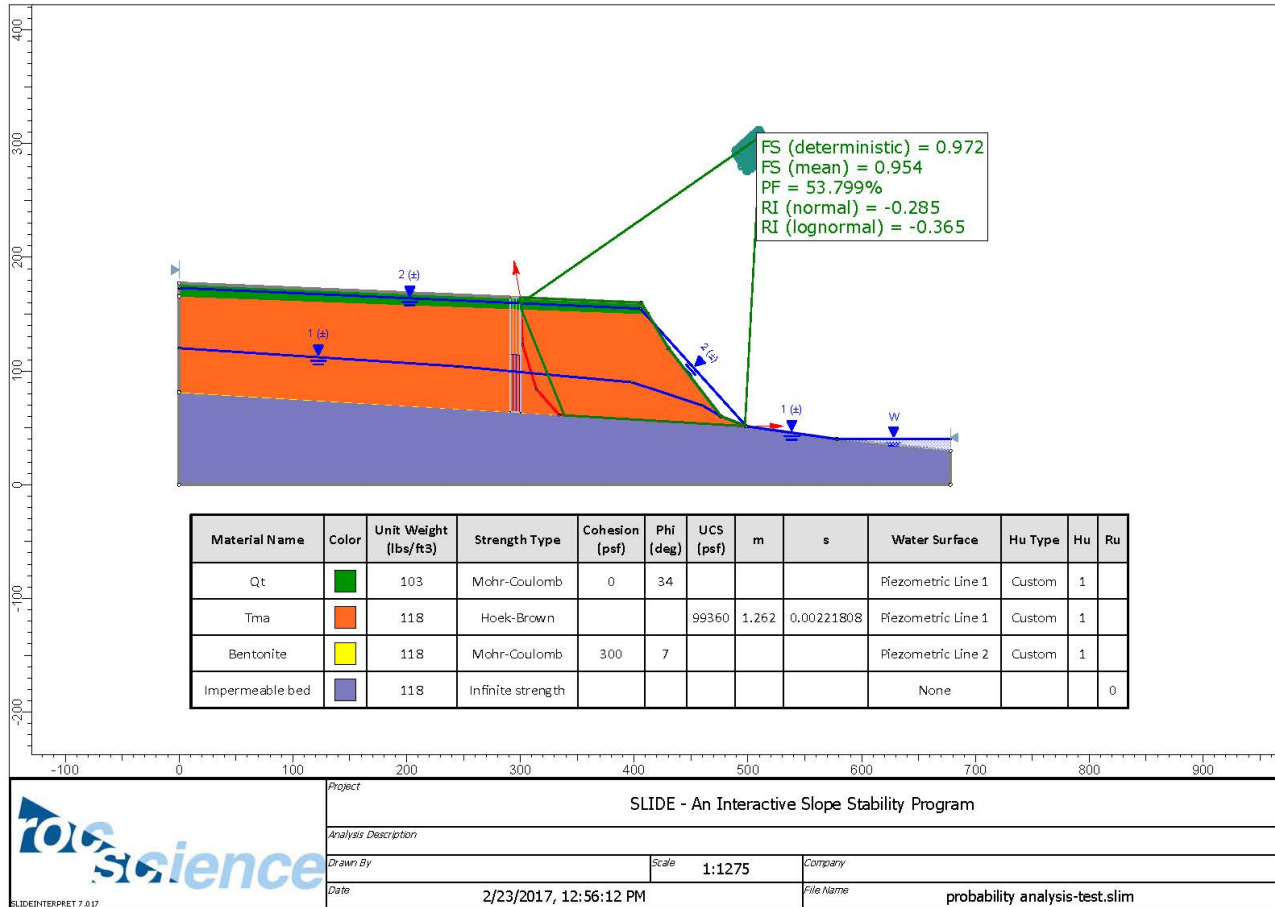


Figure 11 Probabilistic Analysis

6. MITIGATION METHOD

To recover the normal function of the Paso Del Mar before landslide, mitigation methods are discussed below. However, as requested to not to hurt the rock, tie backs are not an option for repairment. In this report, the landslide section is re-filled with a new engineering fill to stabilize the area. Furthermore, when removing the unstable material, excess pore water pressure will be dewatered and drainage materials are suggested to be installed before the placement of engineering fill.

Therefore, the existing piezometric line is lowered due to this consideration, and the confined aquifer phenomenon is eliminated.

The new fill material has a property of 40 psf cohesion and 45° friction angle with 133psf unit weight. As the figure show below, static analysis reached a 1.5 factor of safety.

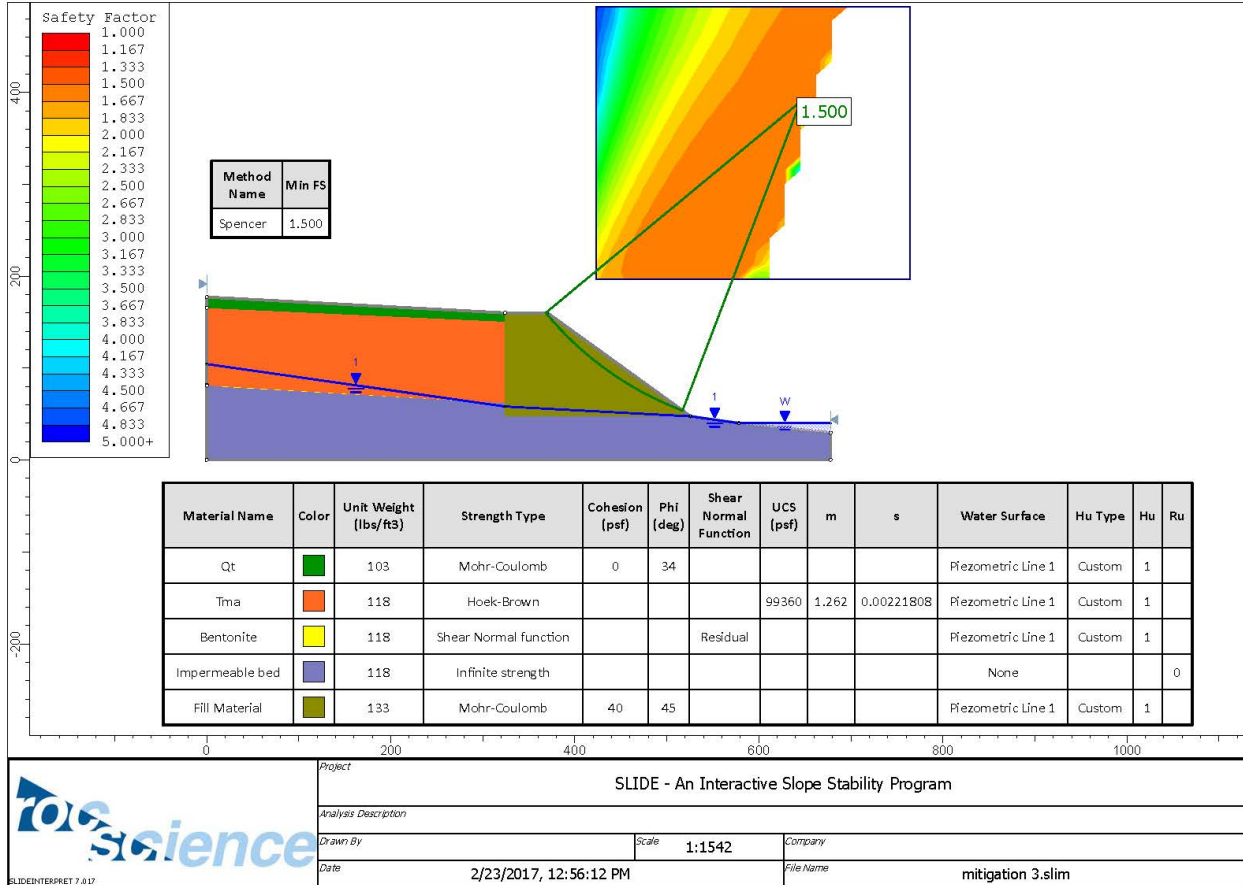


Figure 12 Mitigation Method Analysis

As the top of the new fill will be accomodating the previous road, coordinates of the new section in model is shown below and clearly there is a 46 feet width at top of the section, which would be good enough to place the previous road.

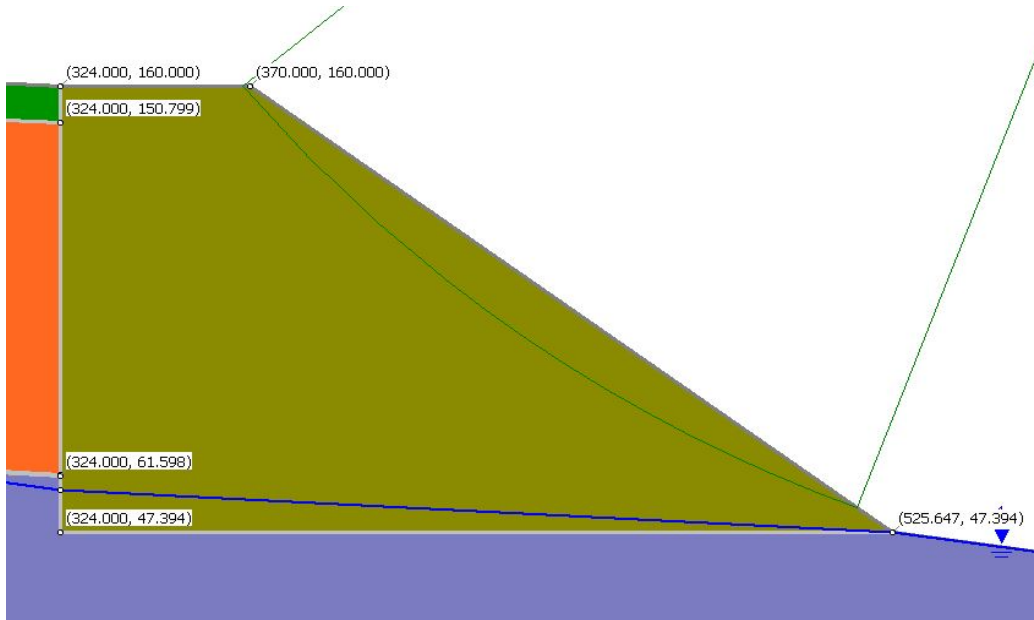


Figure 13 Coordinates of New Fill in Slide7.0

7. SEISMIC HAZARD ANALYSIS

7.1 Static Analysis

With the same model, advanced seismic analysis are performed to compute K_y for $FS=1$, where K_y is the critical yield coefficient. From the result, $K_y = 0.215$

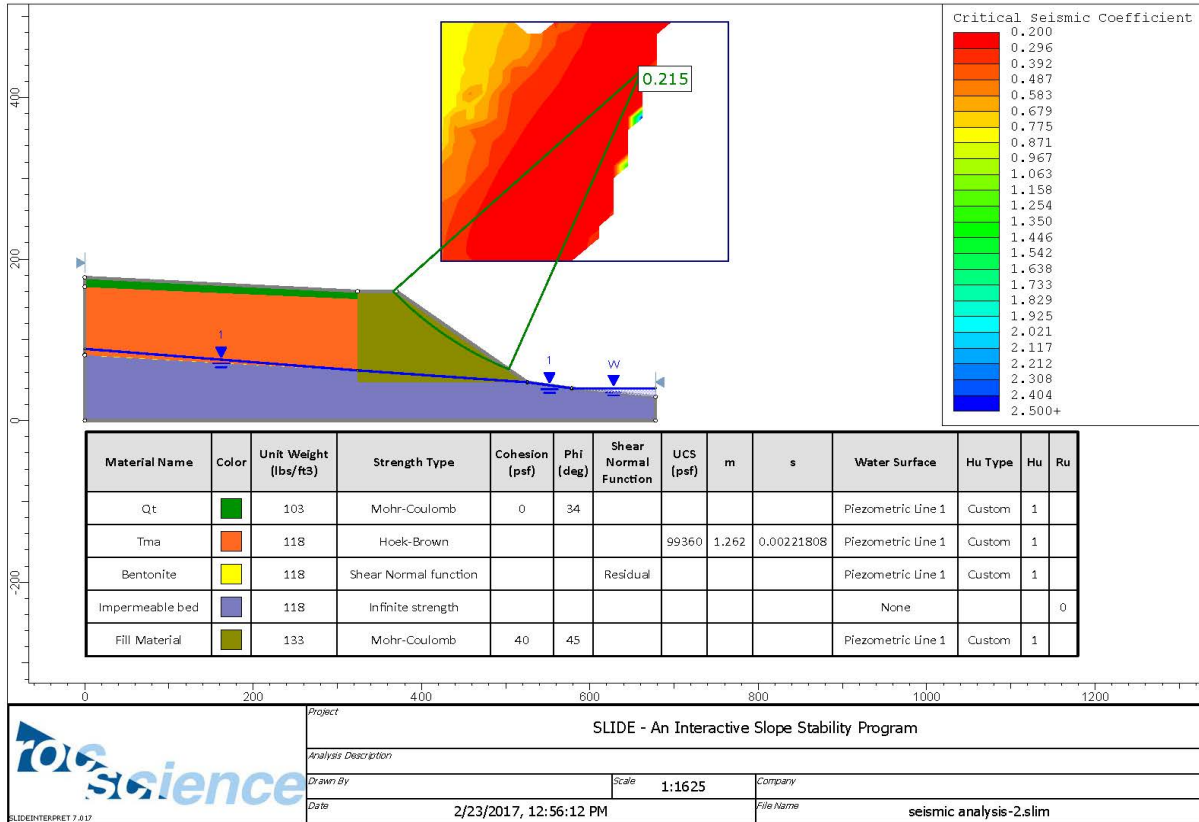


Figure 14 Ky of Static Analysis

7.2 Pseudo-static Analysis

Following the static analysis, Pseudo-static analysis is performed with seismic coefficient to be 0.15 added to horizontal load. As shown below, factor of safety is 1.242 which is larger than 1.1.

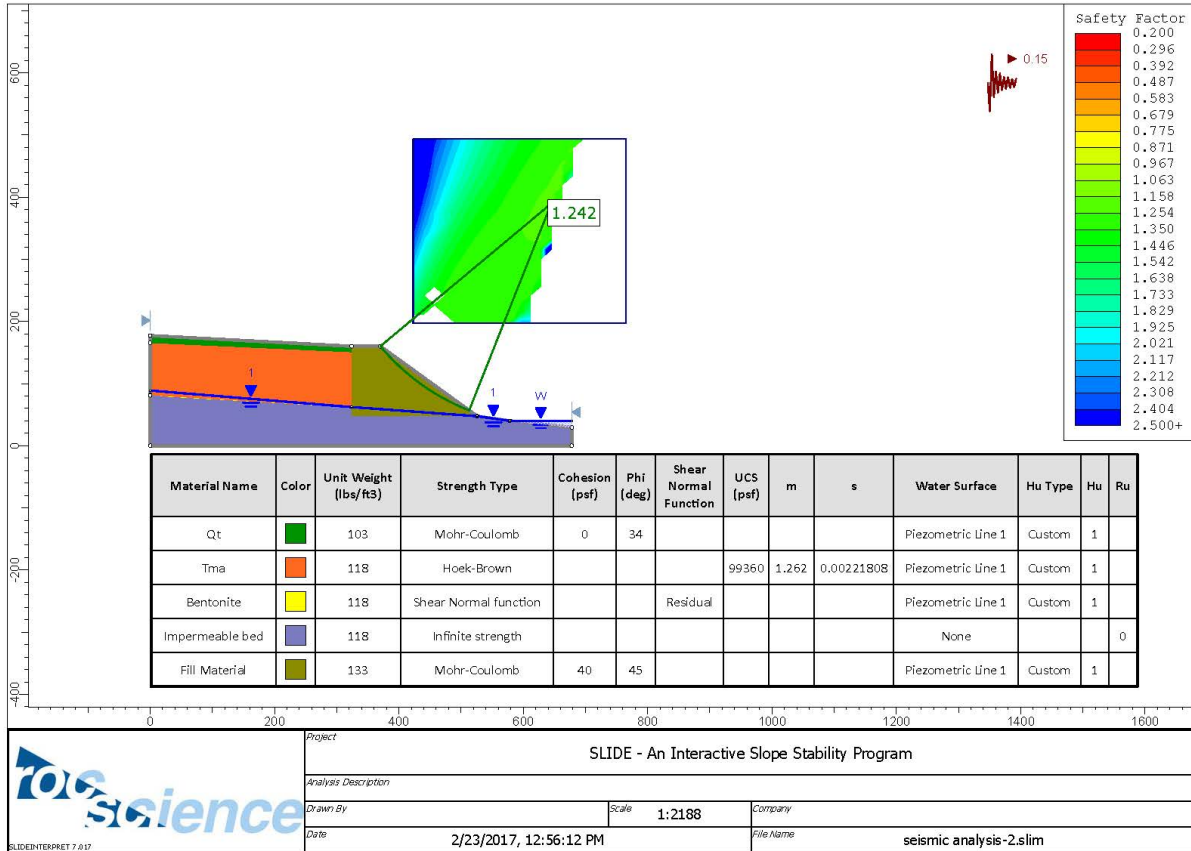


Figure 15 Factor of Safety for Pseudo-static Analysis

7.3 Displacement-Based Analysis

As this site is near the Cabrillo fault, with $R_{jb} = 1.12\text{km}$ and the fault produces earthquake of magnitude 6.7, seismic displacement and corresponding probabilities are calculated.

The height of the new engineered fill is $H = 112.6$ feet (34.3m). V_{s30} are set to be 360m/s, which is a conservative value considering the fill material properties. As this is a 1D analysis,

$$T_s = 4H/V_{s30} = 0.38$$

From the graph below, the corresponding $S_a (g) = 0.9$ g.

As $K_y = 0.215$ from the static analysis, displacements are calculated using Bray and Travararou 2007 as shown in figure and table below. The values shown are of reasonable range for this site.

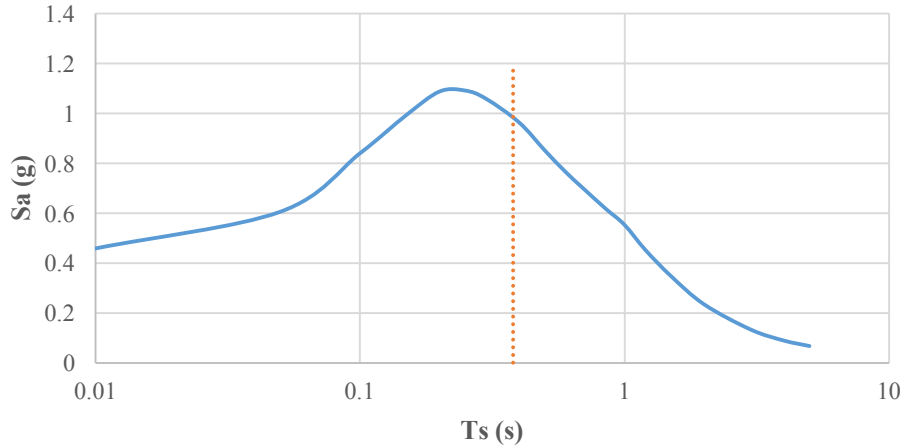


Figure 16 Sa(g) vs. Ts(s) for Cabrillo fault

Simplified Procedure for Estimating Earthquake Induced Deviatoric Slope Displacements		
by Jonathan D. Bray and Thaleia Travarasou		
Journal of Geotechnical and Geoenvironmental Engineering, ASCE, V. 133(4), pp. 381-392, April 2007		
SEE NOTES BELOW FOR GUIDANCE IN THE USE OF SPREADSHEET		
Input Parameters		
Yield Coefficient (ky)	0.215	Based on pseudostatic analysis
Initial Fundamental Period (Ts)	0.38 seconds	1D: Ts=4H/Vs 2D: Ts=2.6H/Vs
Degraded Period (1.5Ts)	0.57 seconds	
Moment Magnitude (Mw)	6.7	
Spectral Acceleration (Sa(1.5Ts))	0.9 g	
Additional Input Parameters		
Probability of Exceedance #1 (P1)	84%	
Probability of Exceedance #2 (P2)	50%	
Probability of Exceedance #3 (P3)	16%	
Displacement Threshold (d_threshold)	30 cm	
Intermediate Calculated Parameters		
Non-Zero Seismic Displacement Est (D)	15.16 cm	eq. (5) or (6)
Standard Deviation of Non-Zero Seismic D	0.66	
Results		
Probability of Negligible Displ. (P(D=0))	0.00	eq. (3)
D1	7.8 cm	calc. using eq. (7)
D2	15.1 cm	calc. using eq. (7)
D3	29.2 cm	calc. using eq. (7)
P(D>d_threshold)	0.15	eq. (7)

Figure 17 Excel for Calculation of Seismic Displacement

Table 5 Seismic Displacement and Corresponding Probability

	Probability of Exceedance	Displacement (cm)
1	84%	7.8
2	50%	15.1
3	16%	29.2

REFERENCES

1. Deane, R. Travis, P.E., G.E. Final Geotechnical Report White Point Landslide. Rep. no. W.O. E1907483. Los Angeles: Shannon and Wilson, 2012. City of Los Angeles Bureau of Engineering. Web. 16 Mar. 2017.
2. Bray, Jonathan D., and Thaleia Travasarou. "Pseudo-static coefficient for use in simplified seismic slope stability evaluation." *Journal of geotechnical and geo-environmental engineering* 135.9 (2009): 1336-1340.
3. Williams, Robert A., William J. Stephenson, Jack K. Odum, and David M. Worley. *High-Resolution Surface-Seismic Imaging Techniques for NEHRP Soil Profile Classifications and Earthquake Hazard Assessments in Urban Areas*. Rep. Golden: United States Geologic Survey, 1997. United States Geologic Survey. Web. 16 Mar. 2017.
4. Yee, Hilton L., P.E. Paseo Del Mar (White Point) Permanent Restoration Project. Rep. Los Angeles: AECOM, 2016. City of Los Angeles Bureau of Engineering. Web. 16 Mar. 2017.
5. Hoek, E. and Brown, E.T. 1980. Empirical strength criterion for rock masses. *J. Geotech. Engng Div., ASCE* 106 (GT9), 1013-1035.

APPENDIX

Bedding Inclination Model Results

